

## Engineered $\epsilon$ -decalactone lipomers by-pass the liver to selectively *in vivo* mRNA delivery to the lungs without targeting ligands

Mahmoud M. Abd Elwakil, Tianle Gao, Takuya Isono, Yusuke Sato, Yaser H. A. Elewa, Toshifumi Satoh and Hideyoshi Harashima

### Materials and Methods:

$\epsilon$ -Decalactone (DL; Sigma-Aldrich,  $\geq 99\%$ ),  $\epsilon$ -caprolactone, 2-(dimethylamino)ethanol (AA01; Tokyo Chemical Industry Co., Ltd. (TCI),  $>99.0\%$ ), *N*-methyldiethanolamine (AA03; TCI,  $>99.0\%$ ), and 2-[[2-(dimethylamino)ethyl]methylamino]ethanol (AA04; TCI,  $>97.0\%$ ) were purified by distillation with  $\text{CaH}_2$  under reduced pressure, and preserved in the glovebox. Methyl acrylate (TCI,  $>99.0\%$ ), lithium aluminum hydride ( $\text{LiAlH}_4$ ; TCI,  $>95.0\%$ ), didecylamine (A02; TCI,  $>97.0\%$ ), ethylenediamine anhydrous (A05; TCI,  $>98.0\%$ ), 3,3'-diaminodipropylamine (A06; TCI,  $>98.0\%$ ), tris(2-aminoethyl)amine (A07; TCI,  $>98.0\%$ ), 1-(2-aminoethyl)pyrrolidine (A08; Sigma-Aldrich, 98%), 1,4-bis(3-aminopropyl)piperazine (A10; TCI,  $>98.0\%$ ), and homopiperazine (A11, TCI,  $>98.0\%$ ) were used as received. *t*-Bu-P<sub>4</sub> (in hexane as  $\sim 0.8 \text{ mol L}^{-1}$  solution; Sigma-Aldrich Chemicals), 1,5,7-triazabicyclo [4.4.0] dec-5-ene (TBD; TCI,  $>98.0\%$ ), and 1,4-bis(2-hydroxyethyl)piperazine (AA09; TCI,  $>98.0\%$ ) were preserved in the glovebox and used as received. Lipofectamine 2000 transfection reagent was purchased from Thermo Fisher Scientific (Cambridge, MA, USA). EGFP and luciferase encoding mRNAs were purchased from TriLink Biotechnologies (San Diego, CA). DMG-PEG<sub>2k</sub> was purchased from NOF corporation, Tokyo, Japan. Cholesterol and DiD were purchased from Sigma. 1,2-Dioleoyl-sn-glycero-3-phosphoethanolamine (DOPE) was purchased from Avanti polar lipids.

### Instruments:

The size exclusion chromatography (SEC) in THF ( $1.0 \text{ mL min}^{-1}$ ) was performed at  $40^\circ\text{C}$  utilized with Shodex 3 GPC-101 system which fit out with a shodex K-G guard column and a set of two Shodex KF-804L columns (linear,  $8 \text{ mm} \times 300 \text{ mm}$ ; bead size,  $5 \mu\text{m}$ ; exclusion limit,  $4 \times 10^6 \text{ g mol}^{-1}$ ). The molecular weight ( $M_{n,\text{SEC}}$ ) and dispersity ( $D$ ) of the measured polymer were calculated by using polystyrene standard curve ranging from 1,200 to 1,320,000  $\text{g mol}^{-1}$ . A JEOL JNMECS400 instrument provided the  $^1\text{H}$  and  $^{13}\text{C}$  NMR spectrum. Transmission electron microscopy (TEM) was performed using a JEM-3200FS electron microscope (JEOL) with an accelerating voltage of 100 kV. For sample preparation, a drop of formulated NP was placed on

a carbon film covered TEM grid, stained with 2% phosphotungestic acid and excess liquid was then wicked by filter paper.. Particle sizes and surface charge were measured by dynamic light scattering (DLS) using a Malvern Zetasizer Nano ZS (He-Ne laser,  $\lambda = 632$  nm).

### Synthesis and characterization of custom initiators:

Amino alcohol initiators were synthesized in two-steps and characterized as previously reported<sup>1</sup> (Figure S1). In brief, amino alcohols A05 (2.00 g, 33.3 mmol, 1 equiv) were dissolved in dry MeOH (21 mL) and placed in a two-neck flask, degassed by argon bubbling for 30 minutes at room temperature and covered with aluminum film to prevent polymerization of methyl acrylate. Methyl acrylate (15.0 mL, 166 mmol, 5 equiv) was added dropwise to this solution. The reaction mixture was stirred at room temperature under inert atmosphere for 2 days. The solvent was removed under reduced pressure to give ester which was then taken directly to the next reduction step. Subsequently, the produced ester (12.0 g, 29.7 mmol, 1 equiv) was dissolved in anhydrous THF (30 mL) and the reaction flask was cooled to 0 °C. The solution was stirred for 30 min at 0 °C under argon atmosphere. Then, LiAlH<sub>4</sub> (6.30 g, 166 mmol, 5.60 equiv) was added into flask very slowly. The mixture was stirred for 48h at room temperature. The reaction was quenched by adding H<sub>2</sub>O (6.3 mL) very slowly at 0 °C. Additionally, NaOH solution (15 wt%, 6.1 mL) was added into the mixture and stirred until all gray solid turned white. After adding H<sub>2</sub>O (18.9 mL), the mixture was filtered through celite and washed by methanol. In order to completely remove LiOH, the product was solubilized in *n*-butanol where LiOH was removed by ultracentrifugation (15000 rpm, 15 min at 20°C, and *n*-butanol was removed by co-evaporation with toluene to give AA05 as yellow liquid (1.70 g, 5.8 mmol, yield: 17.4%).

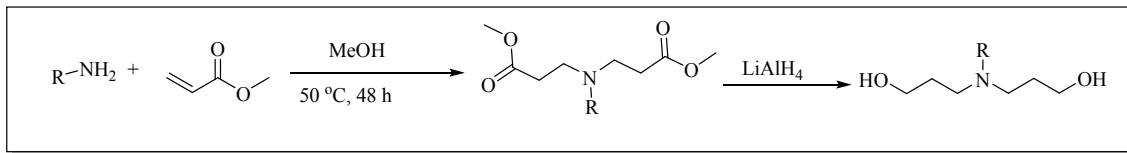


**Figure S1.** Schematic synthesis of custom-made alcohol initiators.

**AA02:** <sup>1</sup>H-NMR (400 MHz, METHANOL-D<sub>4</sub>):  $\delta$  (ppm) 4.90 (s, 1H, -OH), 3.60 (t,  $J = 6.2$  Hz, 2H, -CH<sub>2</sub>OH), 2.55 (t,  $J = 7.3$  Hz, 2H, -NCH<sub>2</sub>-), 2.40-2.44 (m, 4H, -NCH<sub>2</sub>-), 1.63-1.69 (m, 2H, -CH<sub>2</sub>-), 1.28-1.49 (m, 32H, -NCH<sub>2</sub>(CH<sub>2</sub>)<sub>8</sub>CH<sub>3</sub>), 0.89 (t,  $J = 6.9$  Hz, 6H, -CH<sub>3</sub>).

**AA06:**  $^1\text{H}$ -NMR (400 MHz, METHANOL- $\text{D}_4$ ):  $\delta$  (ppm) 5.06 (s, 5H, -OH), 3.65 (td,  $J = 6.2, 3.0$  Hz, 10H, - $\text{CH}_2\text{OH}$ ), 2.61 (t,  $J = 7.3$  Hz, 10H, - $\text{NCH}_2$ -), 2.51 (dt,  $J = 10.4, 4.2$  Hz, 8H, - $\text{NCH}_2$ -), 1.68-1.77 (m, 14H, - $\text{CH}_2$ -).

**AA08:**  $^1\text{H}$ -NMR (400 MHz, METHANOL- $\text{D}_4$ ):  $\delta$  (ppm) 5.27 (s, 2H, -OH), 3.59 (t,  $J = 6.2$  Hz, 4H, - $\text{CH}_2\text{OH}$ ), 2.61 (s, 4H, - $\text{NCH}_2$ -), 2.53-2.58 (m, 8H, - $\text{NCH}_2$ -), 1.78 (td,  $J = 6.6, 3.4$  Hz, 4H, - $\text{CH}_2$ -), 1.64-1.71 (m, 4H, - $\text{CH}_2$ -).

**AA10:**  $^1\text{H}$ -NMR (400 MHz, METHANOL- $\text{D}_4$ ):  $\delta$  (ppm) 5.21 (s, 4H, -OH), 3.61 (t,  $J = 6.2$  Hz, 8H, - $\text{CH}_2\text{OH}$ ), 2.57 (t,  $J = 7.3$  Hz, 12H, - $\text{NCH}_2$ -), 2.48 (t,  $J = 7.3$  Hz, 8H, - $\text{NCH}_2$ -), 2.37 (t,  $J = 7.5$  Hz, 4H, - $\text{NCH}_2$ -), 1.66-1.72 (m, 12H, - $\text{CH}_2$ -).

**AA11:**  $^1\text{H}$ -NMR (400 MHz, METHANOL- $\text{D}_4$ ):  $\delta$  (ppm) 5.11 (s, 2H, -OH), 3.61 (t,  $J = 6.2$  Hz, 4H, - $\text{CH}_2\text{OH}$ ), 2.72-2.75 (m, 8H, - $\text{NCH}_2$ -), 2.59 (t,  $J = 7.5$  Hz, 4H, - $\text{NCH}_2$ -), 1.82 (t,  $J = 5.9$  Hz, 2H, - $\text{CH}_2$ -), 1.70 (dt,  $J = 14.6$  Hz, 6.3 Hz, 4H, - $\text{CH}_2$ -).

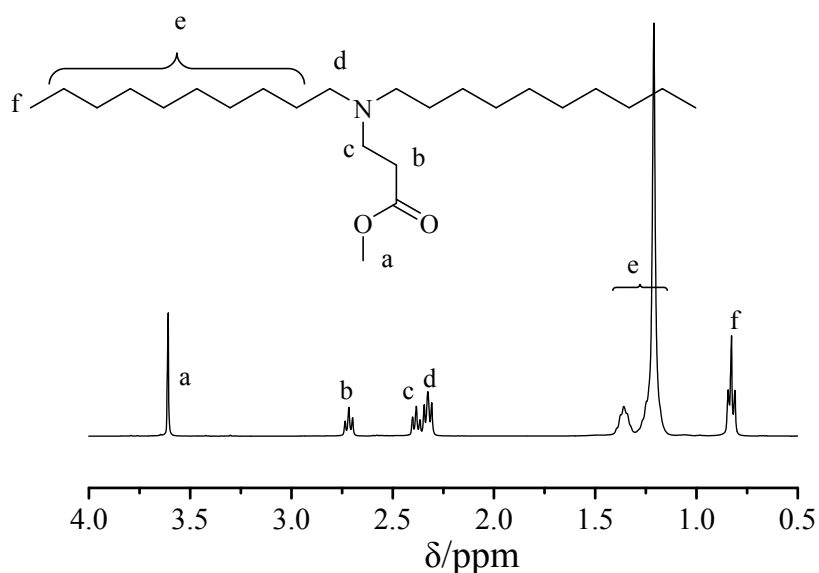


**Figure S2.**  $^1\text{H}$  NMR spectrum of A02 ester (400 MHz,  $\text{CDCl}_3$ ).

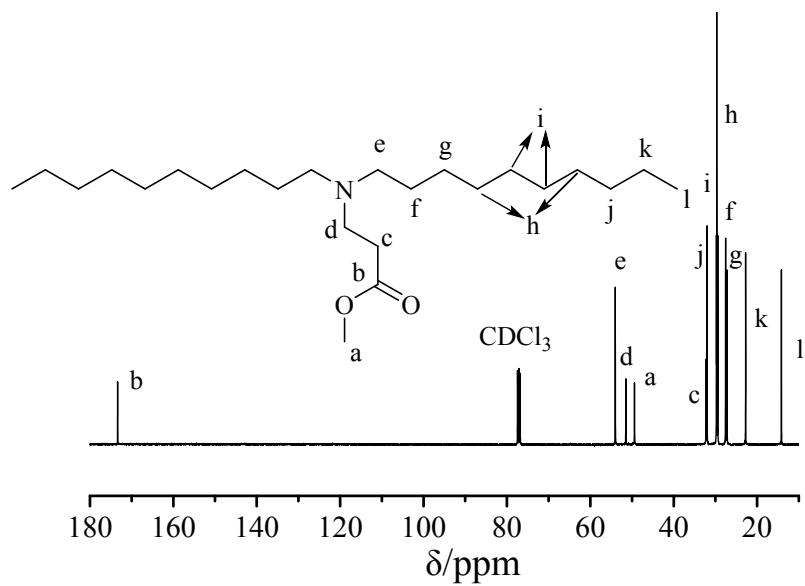


**Figure S3.**  $^{13}\text{C}$  NMR spectrum of A02 ester (100 MHz,  $\text{CDCl}_3$ ).

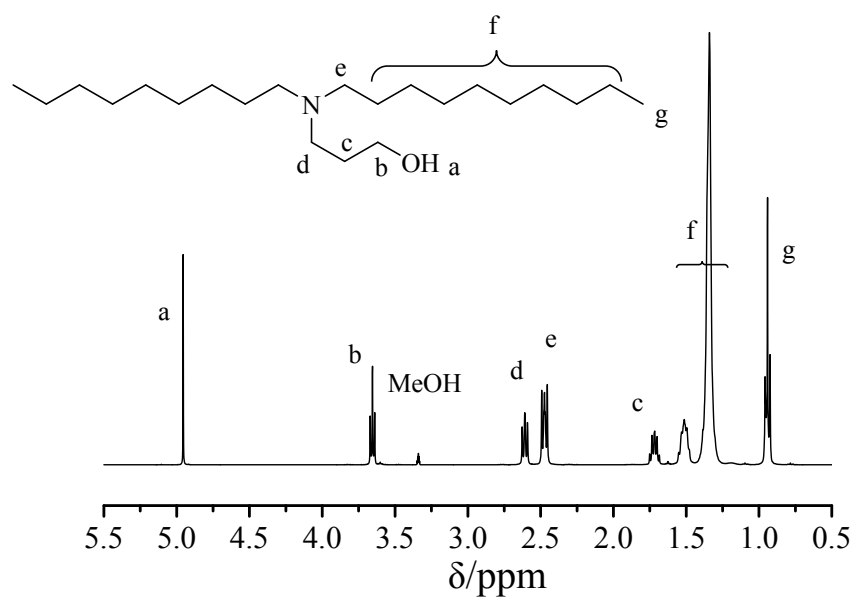


**Figure S4.**  $^1\text{H}$  NMR spectrum of AA02 initiator (400 MHz,  $\text{CD}_3\text{OD}$ ).

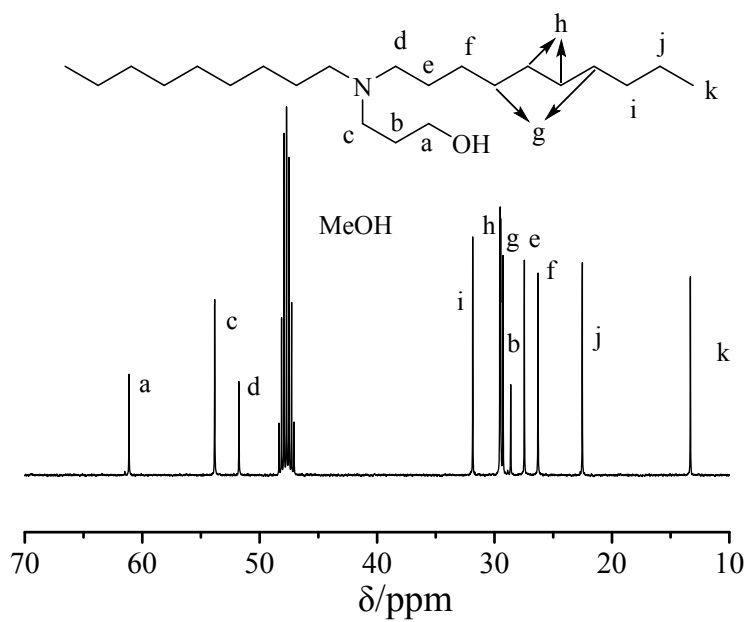


**Figure S5.**  $^{13}\text{C}$  NMR spectrum of AA02 initiator (100 MHz,  $\text{CD}_3\text{OD}$ ).

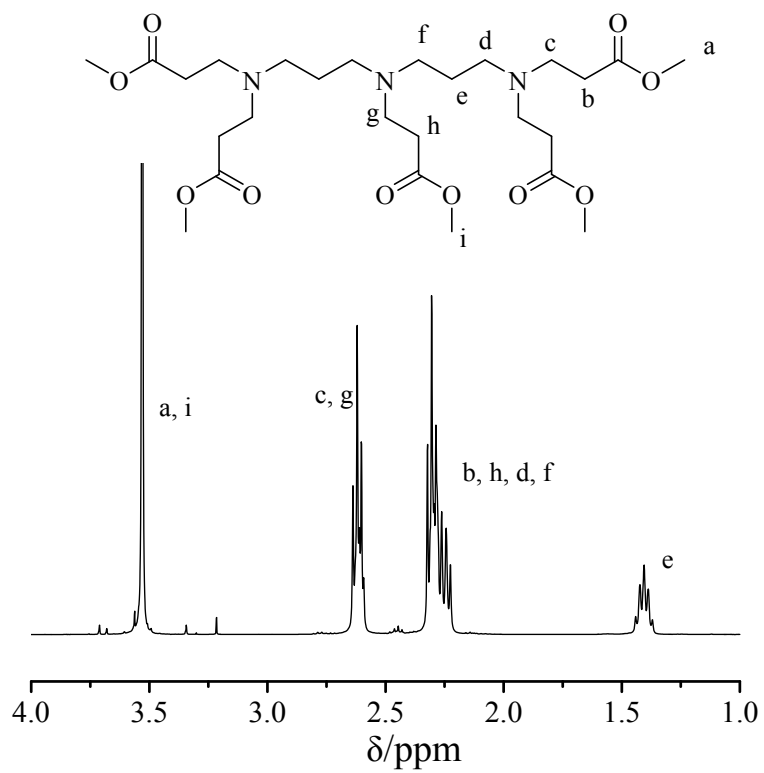


**Figure S6.**  $^1\text{H}$  NMR spectrum of A06 ester (400 MHz,  $\text{CDCl}_3$ ).

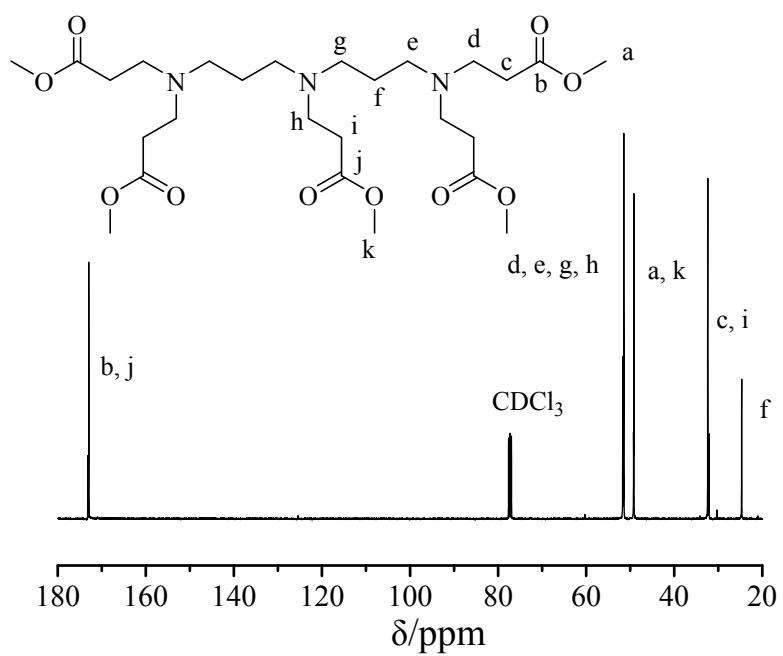


**Figure S7.**  $^{13}\text{C}$  NMR spectrum of A06 ester (100 MHz,  $\text{CDCl}_3$ ).

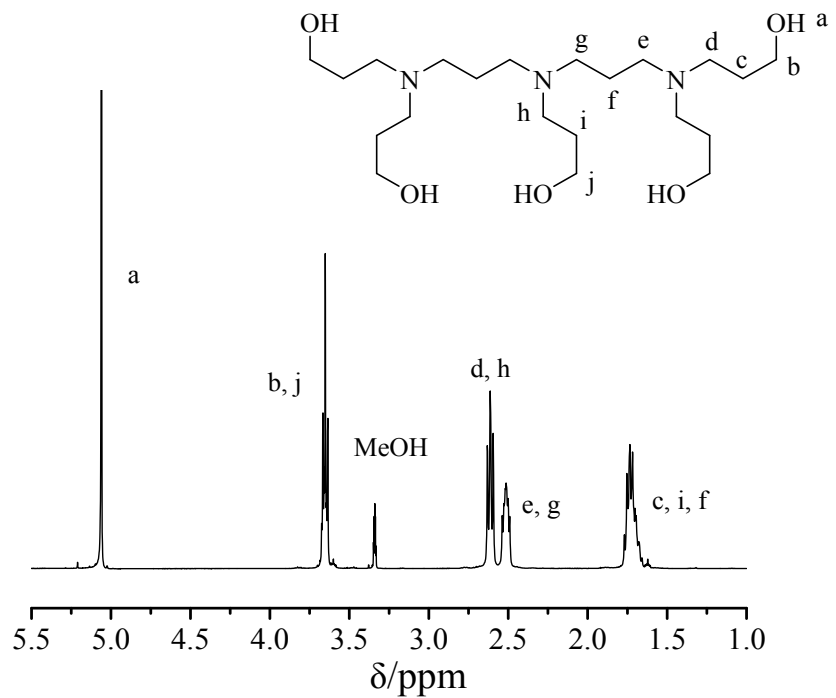


**Figure S8.**  $^1\text{H}$  NMR spectrum of AA06 initiator (400 MHz,  $\text{CD}_3\text{OD}$ ).

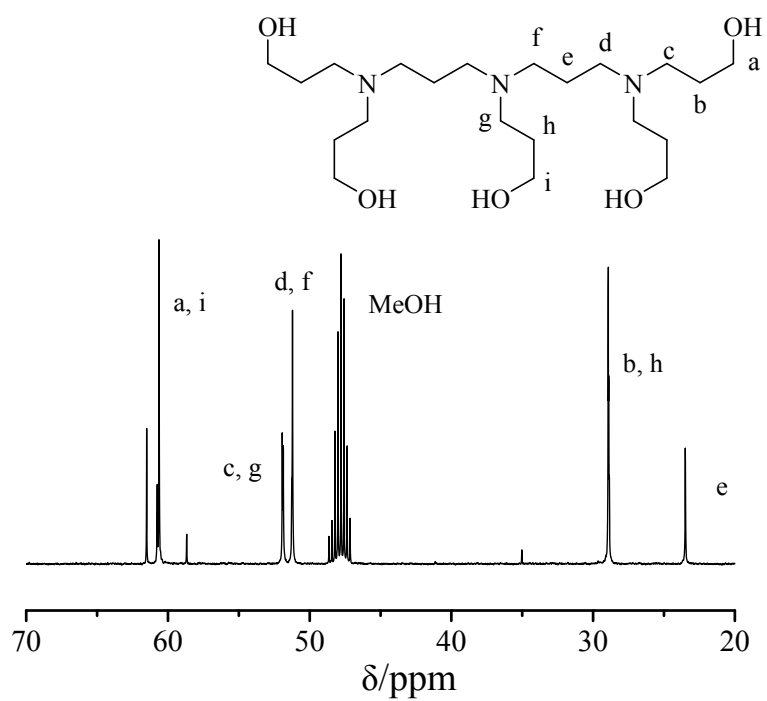


**Figure S9.**  $^{13}\text{C}$  NMR spectrum of AA06 initiator (100 MHz,  $\text{CD}_3\text{OD}$ ).

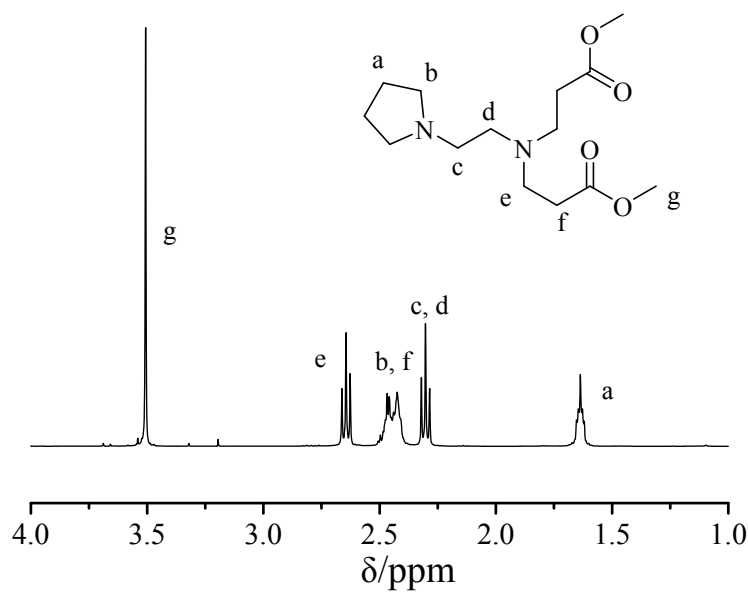


**Figure S10.**  $^1\text{H}$  NMR spectrum of A08 ester (400 MHz,  $\text{CDCl}_3$ ).

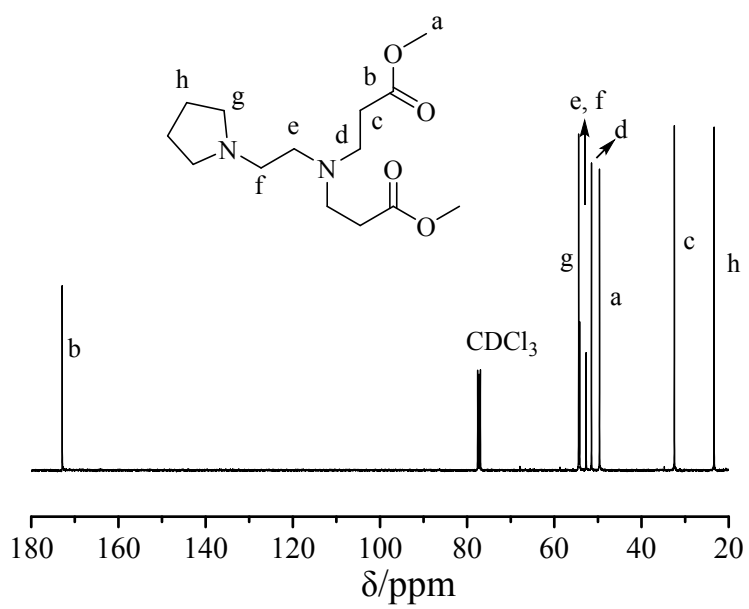


**Figure S11.**  $^{13}\text{C}$  NMR spectrum of A08 ester (100 MHz,  $\text{CDCl}_3$ ).

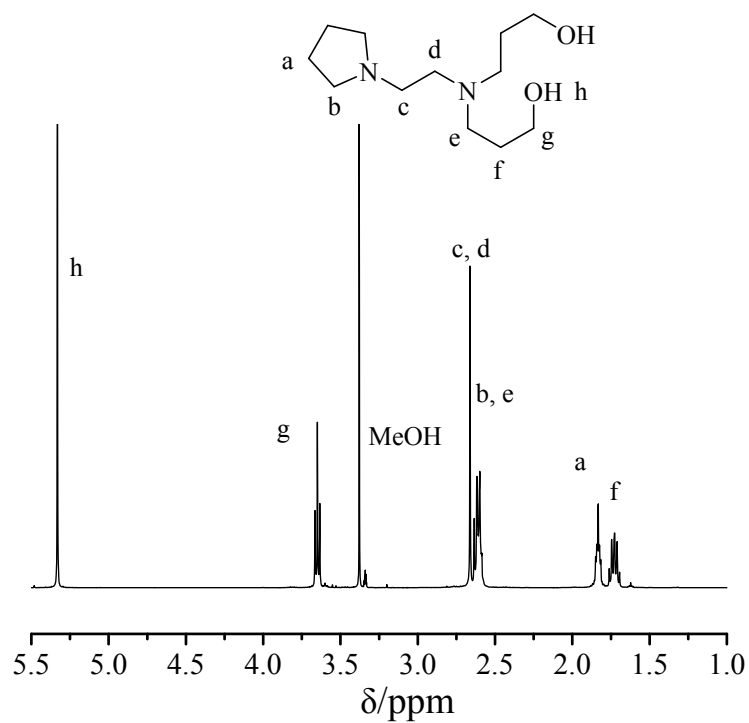


**Figure S12.**  $^1\text{H}$  NMR spectrum of AA08 initiator (400 MHz,  $\text{CD}_3\text{OD}$ ).

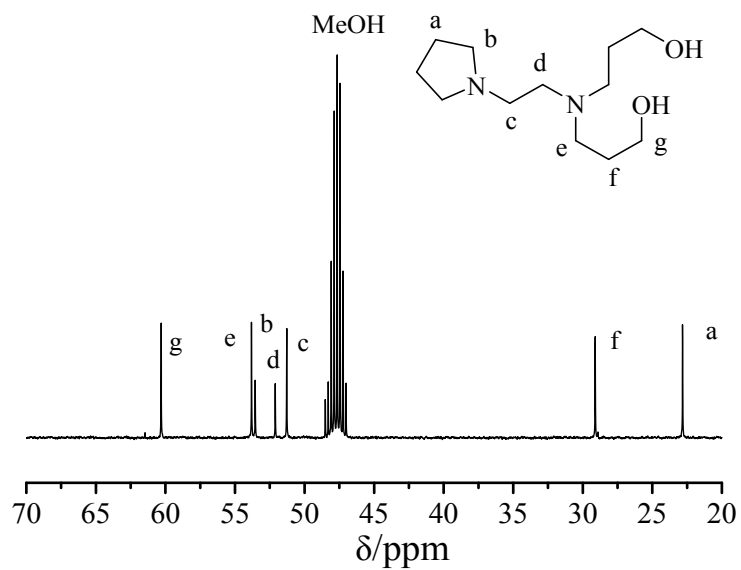


**Figure S13.**  $^{13}\text{C}$  NMR spectrum of AA08 initiator (100 MHz,  $\text{CD}_3\text{OD}$ ).

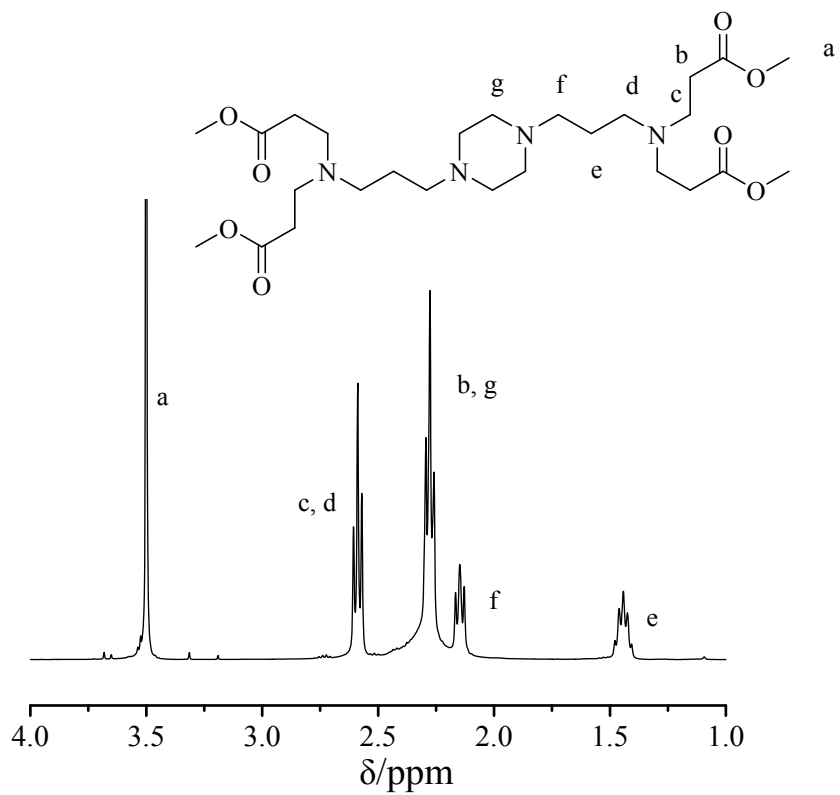


**Figure S14.**  $^1\text{H}$  NMR spectrum of A10 ester (400 MHz,  $\text{CDCl}_3$ ).

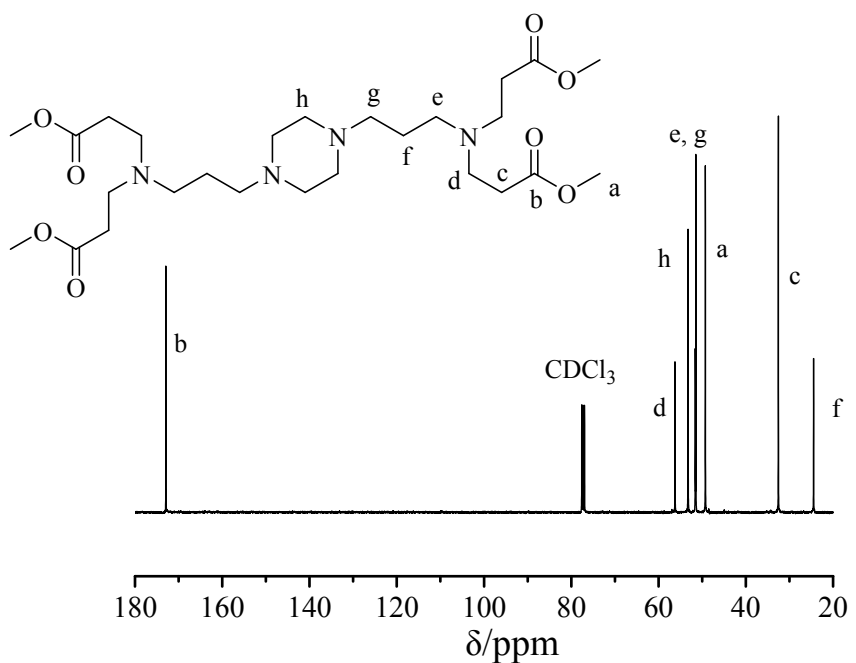


**Figure S15.**  $^{13}\text{C}$  NMR spectrum of A10 ester (100 MHz, CDCl<sub>3</sub>).

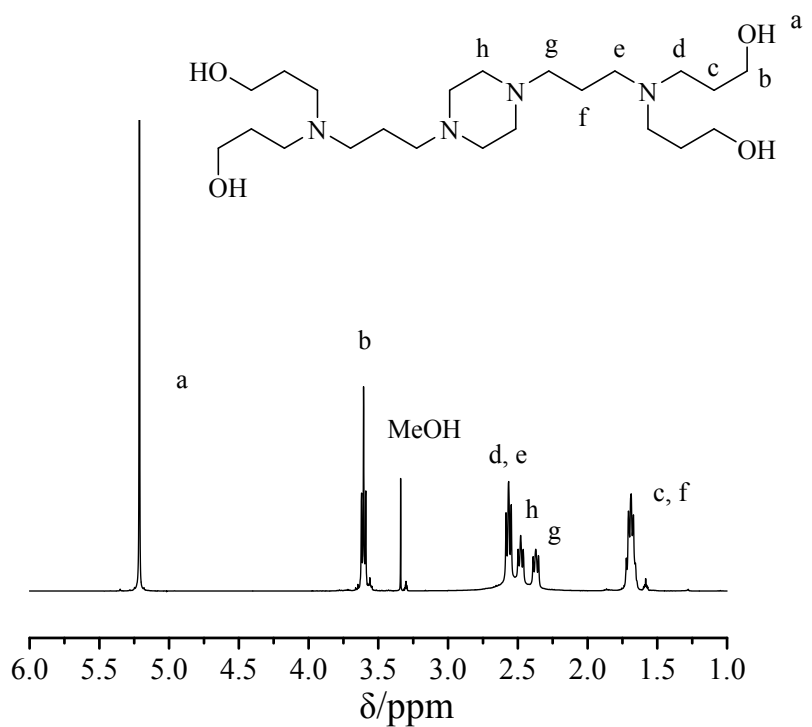


**Figure S16.**  $^1\text{H}$  NMR spectrum of AA10 initiator (400 MHz, CD<sub>3</sub>OD).

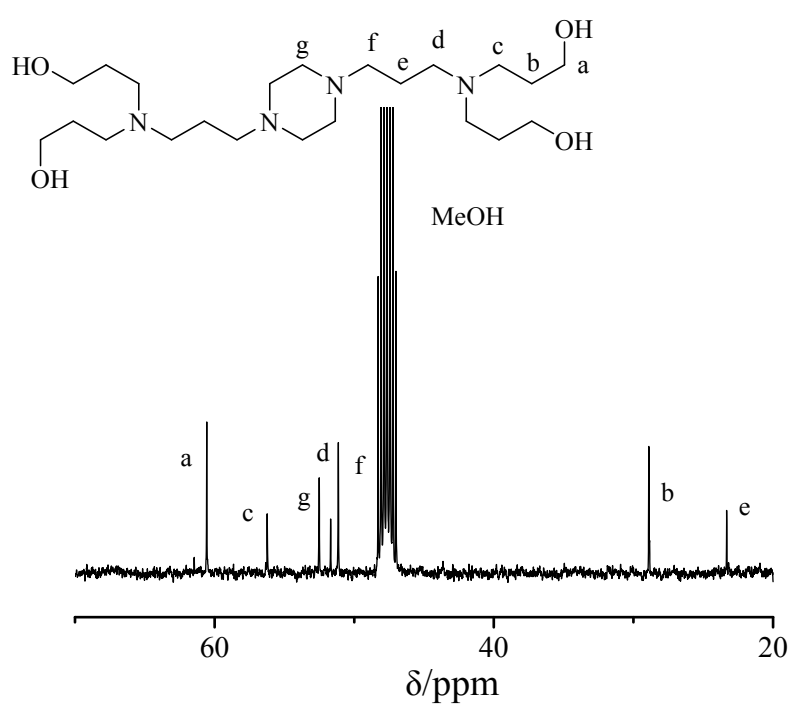


**Figure S17.**  $^{13}\text{C}$  NMR spectrum of AA10 initiator (100 MHz,  $\text{CD}_3\text{OD}$ ).

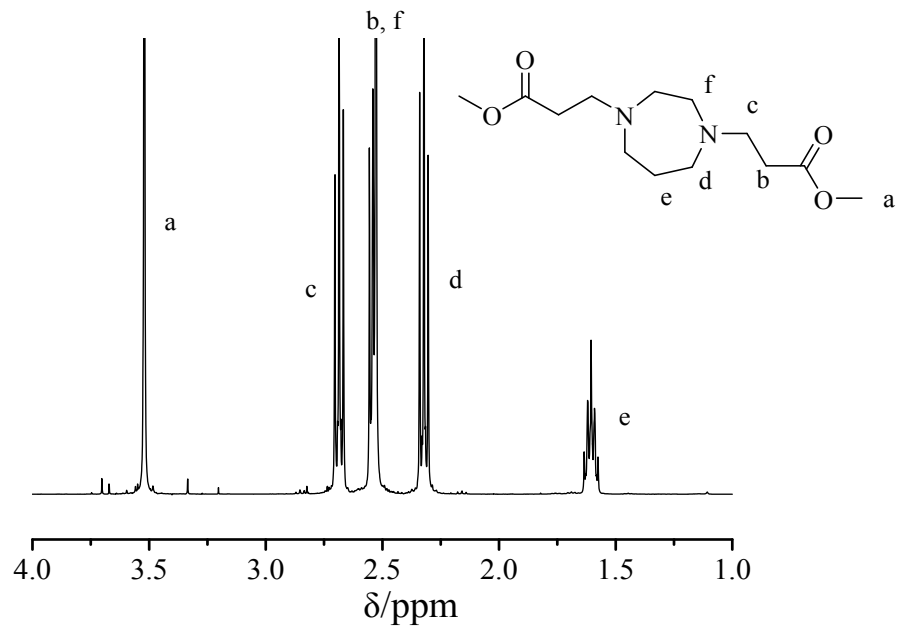


**Figure 18.**  $^1\text{H}$  NMR spectrum of A11 ester (400 MHz,  $\text{CDCl}_3$ ).

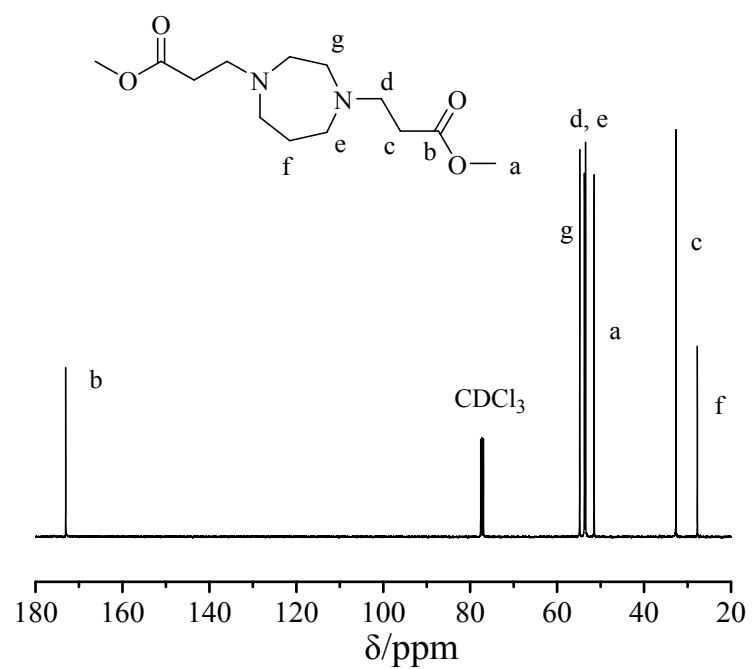


**Figure S19.**  $^{13}\text{C}$  NMR spectrum of A11 ester (100 MHz, CDCl<sub>3</sub>).

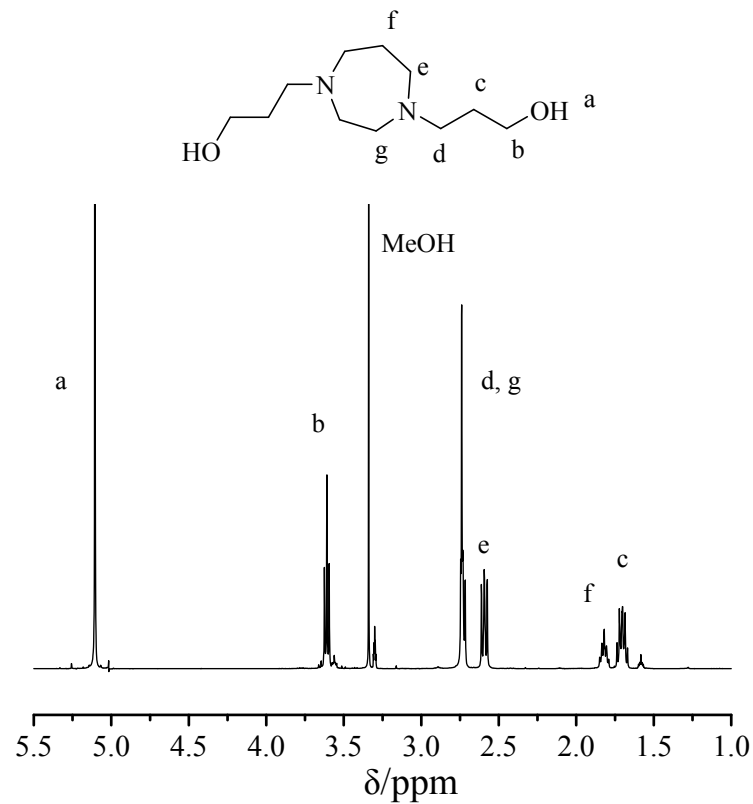


**Figure S20.**  $^1\text{H}$  NMR spectrum of AA11 initiator (400 MHz, CD<sub>3</sub>OD).

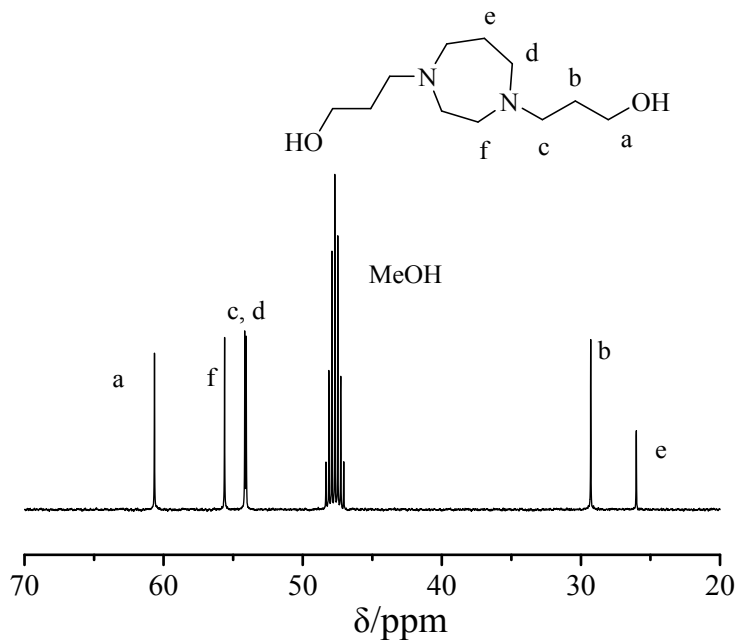


**Figure S21.**  $^{13}\text{C}$  NMR spectrum of AA11 initiator (100 MHz,  $\text{CD}_3\text{OD}$ ).

**Synthesis and characterization of CL and DL lipomers:**

The  $\varepsilon$ -CL and  $\varepsilon$ -DL polymers were synthesized via ring-opening polymerization (ROP) of  $\varepsilon$ -CL/ $\varepsilon$ -DL in the presence of different amino alcohols as initiators and different catalyst in toluene at room temperature. Therefore, we investigated four different organocatalysts, diphenyl phosphate (DPP), triazabicyclodecene (TBD) and phosphazene bases  $t\text{-BuP}_1$  and  $t\text{-BuP}_4$  catalysts in toluene. A kinetic study showed that  $t\text{-BuP}_4$  catalyst achieved steady forward synthesis of monodisperse  $\varepsilon$ -DL polymers in short time. The monomer to the initiator hydroxyl group ratio was set equal to the desired degree of polymerization in order to obtain lipomers with 3, 5 and 10 kDa of lactones for each arm. In the glovebox, initiators,  $\varepsilon$ -DL and  $t\text{-Bu-P}_4$  were mixed in a 15-mL vial with toluene. The reaction was carried out at room temperature while stirring. When monomers conversion ratio reached  $\sim$ 80-90%, benzoic acid was added to quench the reaction. The polymers were purified three times by precipitation in cold methanol then dried overnight, characterized and stored in  $-20^\circ\text{C}$  until further use.

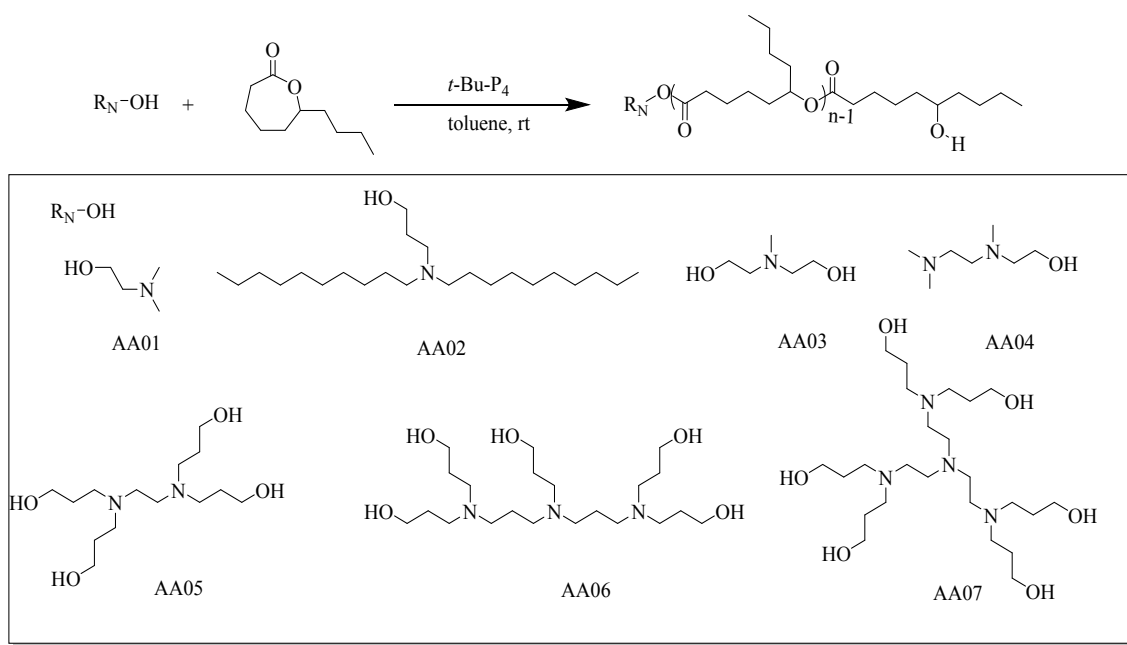


**Figure S22. Schematic synthesis of  $\epsilon$ -DL lipomers using linear amino alcohol initiators.**

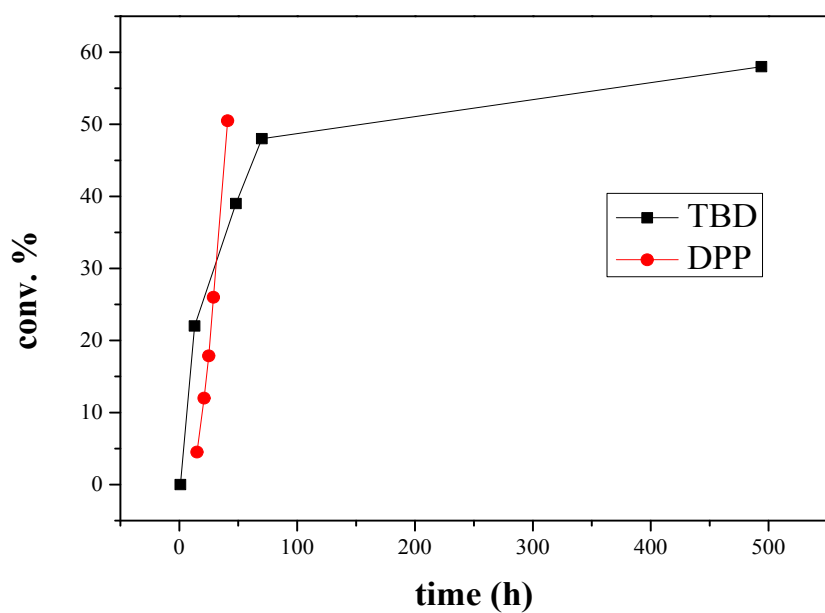


**Figure S23.** Polymerization kinetics of AA01-DL using TBD (black) and DPP (red) as catalyst.

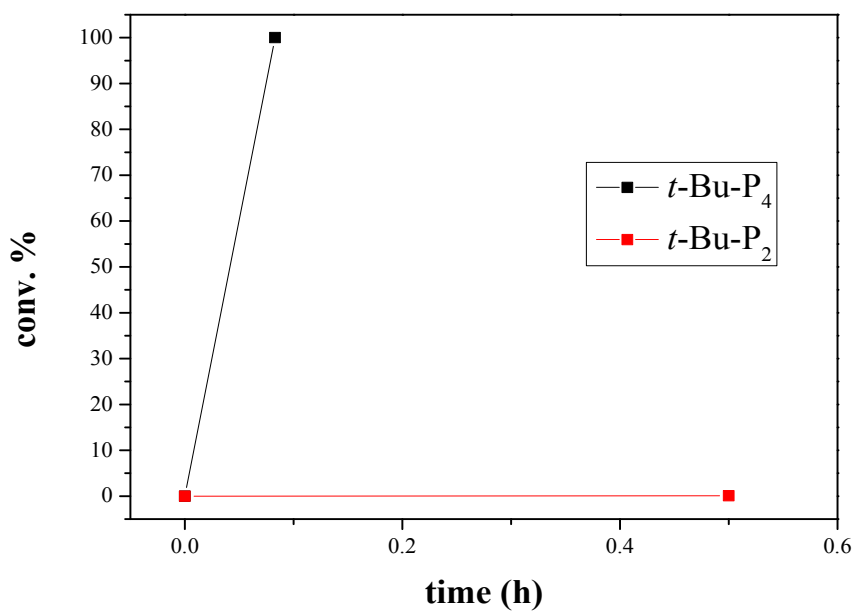


**Figure S24.** Polymerization kinetics of AA01-DL using  $t\text{-Bu-P}_4$  (black) and  $t\text{-Bu-P}_2$  (red) as catalyst.

**Table S1. Molecular characteristics of  $\varepsilon$ -DL polymers prepared by *t*-Bu-P<sub>4</sub>-catalyzed ROP using linear amino alcohol initiator**

Polymer	[M] <sub>0</sub> /[initiator] <sub>0</sub> /[Cat.]	Conv (%) <sup>a</sup>	$M_{n, th}$	$M_{n, NMR}$ <sup>b</sup>	$M_{n, SEC}$ <sup>c</sup>	$D$ <sup>c</sup>
AA01-DL-3	20/1/0.2	85	3400	2900	6400	1.21
AA01-DL-5	30/1/0.2	87	5100	4400	9200	1.18
AA01-DL-10	70/1/0.2	82	11900	9800	13800	1.11
AA02-DL-3	18/1/0.2	93	2800	2900	7600	1.28
AA02-DL-5	30/1/0.2	95	4800	4700	9500	1.38
AA02-DL-10	60/1/0.2	98	10000	9500	14500	1.53
AA03-DL-3	35/1/0.2	89	6000	5300	10200	1.18
AA03-DL-5	60/1/0.2	86	10200	8800	14300	1.12
AA03-DL-10	100/1/2	888	17000	15200	16200	1.17
AA04-DL-3	17/1/0.2	90	2700	2600	10700	1.15
AA04-DL-5	29/1/0.2	93	4600	4700	12000	1.21
AA04-DL-10	59/1/0.2	96	9600	9900	17000	1.32
AA05-DL-3	72/1/1.2	98	12000	12900	12800	1.29
AA05-DL-5	120/1/1.2	97	19800	23100	17600	1.61
AA05-DL-10	240/1/1.2	97	27100	29600	35300	1.71
AA06-DL-3	88/1/1.5	90	13500	12700	14500	1.21
AA06-DL-5	147/1/1.5	97	24200	22900	17300	1.38
AA06-DL-10	295/1/1.5	97	33900	30100	38200	1.67
AA07-DL-3	106/1/1.2	96	17200	30600	19400	1.50
AA07-DL-5	176/1/1.2	94	28200	34700	22400	1.55
AA07-DL-10	352/1/1.2	95	39900	39900	31300	1.74

<sup>a</sup> Calculated by <sup>1</sup> H NMR spectroscopy. <sup>b</sup>  $M_{n, NMR} = [(DP_{NMR}) \times 170.25 \times (MW \text{ of } \varepsilon\text{-DL})] + MW \text{ of initiator}$ . <sup>c</sup>  $M_{n, SEC}$  and  $D$  from polymer after purification, using PS calibration.

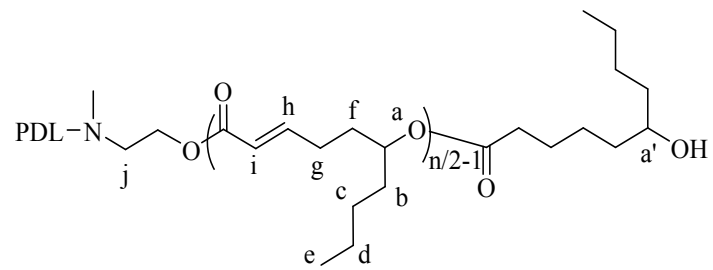


**Figure S25.**  $^1\text{H}$  NMR spectrum of AA03-DL-10 (400 MHz,  $\text{CDCl}_3$ ).

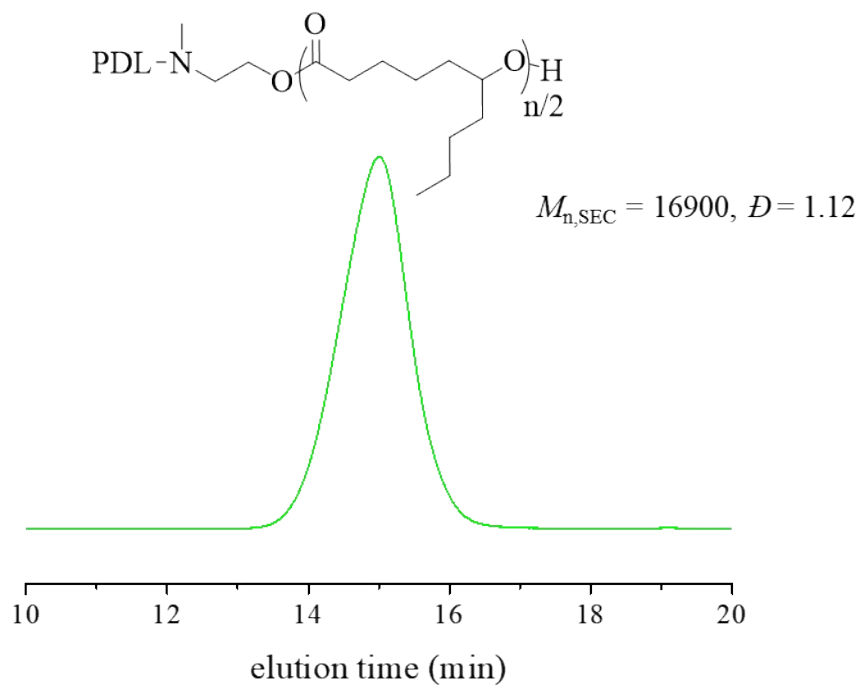


**Figure S26.** SEC traces of AA03-DL-10 (eluent, THF; flow rate, 1.0  $\text{mL min}^{-1}$ ).

**Table S2. Molecular characteristics of  $\varepsilon$ -DL polymers prepared by *t*-Bu-P<sub>4</sub>-catalyzed ROP using cyclic amino alcohol initiator:**

Polymer	[M] <sub>0</sub> /[initiator] <sub>0</sub> /[Cat.]	Conv (%) <sup>a</sup>	<i>M</i> <sub>n, th</sub>	<i>M</i> <sub>n, NMR</sub> <sup>b</sup>	<i>M</i> <sub>n, SEC</sub> <sup>c</sup>	<i>D</i> <sup>c</sup>
AA08-DL-3	36/1/0.4	88	5400	5800	12300	1.18
AA08-DL-5	59/1/0.4	92	9200	8500	14400	1.25
AA08-DL-10	118/1/1	99	19800	17000	16000	1.46
AA09-DL-3	40/1/4	88	6000	5400	9100	1.11
AA09-DL-5	63/1/4	89	9500	10900	11800	1.12
AA09-DL-10	126/1/4	94	20100	17000	13700	1.16
AA10-DL-3	72/1/0.8	88	10800	12900	15100	1.31
AA10-DL-5	118/1/0.8	88	17600	19000	19100	1.51
AA10-DL-10	235/1/2	98	27400	26500	23600	1.37
AA11-DL-3	36/1/0.4	98	6000	6500	14900	1.16
AA11-DL-5	59/1/0.4	99	9900	9500	17600	1.20
AA11-DL-10	118/1/1	99	20100	16000	20700	1.38

<sup>a</sup> Calculated by <sup>1</sup> H NMR spectroscopy. <sup>b</sup> *M*<sub>n, NMR</sub> = [(DP<sub>NMR</sub>) × 170.25 × (MW of  $\varepsilon$ -DL)] + MW of initiator. <sup>c</sup> *M*<sub>n, SEC</sub> and *D* from polymer after purification, using PS calibration.

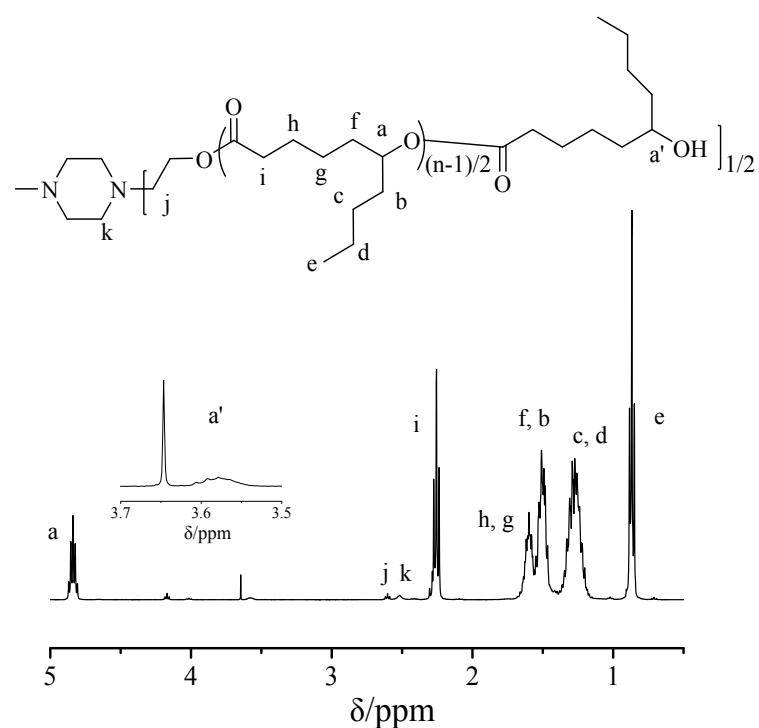


**Figure S27.**  $^1\text{H}$  NMR spectrum of AA09-DL-3 (400 MHz,  $\text{CDCl}_3$ ).

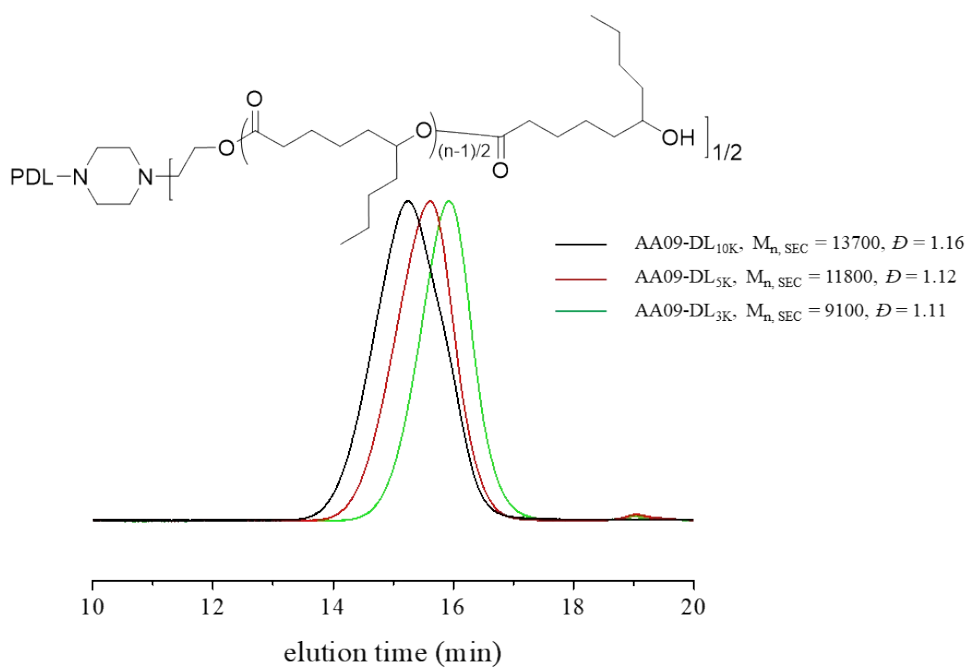


**Figure S28.** SEC traces of AA09-DL-3, 5, 10 (eluent, THF; flow rate,  $1.0 \text{ mL min}^{-1}$ ).

### **Formulation, characterization, and screening of the nanoparticles:**

$\varepsilon$ -CL and  $\varepsilon$ -DL lipomers were formulated by ethanol dilution method. The ethanol phase was prepared by mixing ionizable polymer (in DMF), 1,2-dimyristoyl-sn-glycero-3-phosphoethanolamine-*N*-[methoxy-(polyethyleneglycol)-2000] (ammonium salt) (C14-PEG 2000, Avanti) at a molar ratio of 9:1 and 30:1 lipomer to RNA mass ratio. mRNA encapsulation was analyzed using Quant-iT RiboGreen assay (Thermo Fisher), according to manufacturer's protocol. Nanoparticle size, polydispersity (PDI), and  $\zeta$ -potential were analyzed by dynamic light scattering (DLS) using Zetasizer Nano ZS (Malvern Instruments, Worcestershire, UK). Lipomers hydrodynamic diameters are reported in the percent intensity mode and are an average of three independent measurements. For *in vitro* transfections, HeLa cells (ATCC® CCL-2™) were cultured in Dulbecco's Modified Eagle's Medium (4500 mg L<sup>-1</sup> glucose) supplemented with 10% heat-inactivated fetal bovine serum and penicillin/streptomycin at 37°C and 5% CO<sub>2</sub>. 1x10<sup>5</sup> cells per well were seeded in a 24-well plate (Costar), one day before the experiment. Lipomeric NPs containing 100 ng of EGFP mRNA were added to each well and incubated for 8 h. Cell Viability (MTT assay) and GFP expression were analysed. The fluorescence was quantified using Tecan Infinite M200 Pro plate reader (Tecan US, Morrisville, NC). For *in vivo* screening, ICR mice were intravenously injected with 0.25 mg EGFP mRNA/kg and EGFP fluorescence intensity was quantified 8 hours after injection using FluorVivo imaging system. All animal experimental protocols used in this study were reviewed and approved by the Hokkaido University Animal Care Committee in accordance with the guidelines for the care and use of laboratory animals.

### **Cellular uptake analysis**

For the flow cytometry analysis, Hela cells were seeded at 2x10<sup>5</sup> per well into 12-well plates one day before the experiment and incubated for 3 h with DiD labelled lipomeric NPs. Cells were washed with PBS and detached from the surface using trypsin/EDTA (Sigma, Ayrshire, UK) after which they were immediately transferred to tubes containing 5% FBS (fetal bovine serum, Thermo Fisher) in PBS and kept on ice. Next, samples were centrifuged for 5 min at 220 x g at 4 °C, followed by two washing steps with FACS buffer and suspended in 0.75 mL FACS and were analyzed using CytoFLEX (Beckman Coulter) flow cytometer. For fluorescent microscopy analysis, Hela cells were seeded onto cover glasses placed into 24-well plates at 50,000 cells per well one day before the experiment. Cells were incubated for 8 h with the lipomeric NPs containing 100 ng of EGFP mRNA added to serum-free DMEM. Cells were incubated for 8 h at 37 °C, then media was removed and 1 mL of DMEM was added to wells. GFP fluorescence was acquired using Olympus Microscope with GFP filter set. For cellular uptake mechanism, HeLa cells were incubated with endocytosis inhibitors (2 $\mu$ M Filipin, 20 $\mu$ M

chlorpromazine and 100 $\mu$ M Amiloride) and DiD, EGFP fluorescence was recorded using CytoFLEX (Beckman Coulter) flow cytometer<sup>2,3</sup>.

**Statistical Analysis:** All statistical analyses were performed with GraphPad Prism software. Comparisons between multiple treatments were made utilizing the one-way analysis of variance (ANOVA) followed by Bonferroni or Student–Newman–Keuls test. A *P*-value of  $<0.05$  was considered to be significant.

**Table S3. Physicochemical characterization of  $\epsilon$ -DL lipomers with linear amino alcohol initiators**

Nanoparticle	Particle size (nm)	PdI	$\zeta$ potential (mV)	EE%
AA01-DL-3	345	0.27	-25.6	86
AA01-DL-5	282	0.19	-10.6	87
AA01-DL-10	245	0.22	-15.7	92
AA02-DL-3	423	0.31	-20	84
AA02-DL-5	332	0.27	-25	87
AA02-DL-10	340	0.29	-15.7	88
AA03-DL-3	278	0.32	-24.2	89
AA03-DL-5	246	0.27	-18.7	87
AA03-DL-10	126	0.25	-22.6	90
AA04-DL-3	245	0.21	-33	84
AA04-DL-5	236	0.27	-21	85
AA04-DL-10	261	0.21	-15.5	86
AA05-DL-3	352	0.32	-22.5	83
AA05-DL-5	252	0.31	-17.8	88
AA05-DL-10	262	0.25	-15.7	91
AA06-DL-3	377	0.27	-22.2	84

AA06-DL-5	345	0.22	-18.9	86
AA06-DL-10	247	0.27	-17.2	88
AA07-DL-3	411	0.32	-29	88.7
AA07-DL-5	314	0.35	-22	89.5
AA07-DL-10	316	0.25	-10.5	90.1

**Table S4. Physicochemical characterization of  $\varepsilon$ -DL lipomers with cyclic amino alcohol initiators**

Nanoparticle	Particle size (nm)	PdI	$\zeta$ potential (mV)	EE%
AA08-DL-3	382	0.29	-20.6	87
AA08-DL-5	245	0.22	-15.7	92
AA08-DL-10	230	0.21	-14.2	90
AA09-DL-3	374	0.35	-18.5	84
AA09-DL-5	339	0.27	-13.9	90.5
AA09-DL-10	335	0.29	-11.5	91
AA10-DL-3	317	0.29	-23.7	82
AA10-DL-5	278	0.23	-18.9	87
AA10-DL-10	257	0.27	-15.2	86
AA11-DL-3	360	0.34	-29	85
AA11-DL-5	340	0.27	-21.7	87
AA11-DL-10	224	0.24	-14.7	88

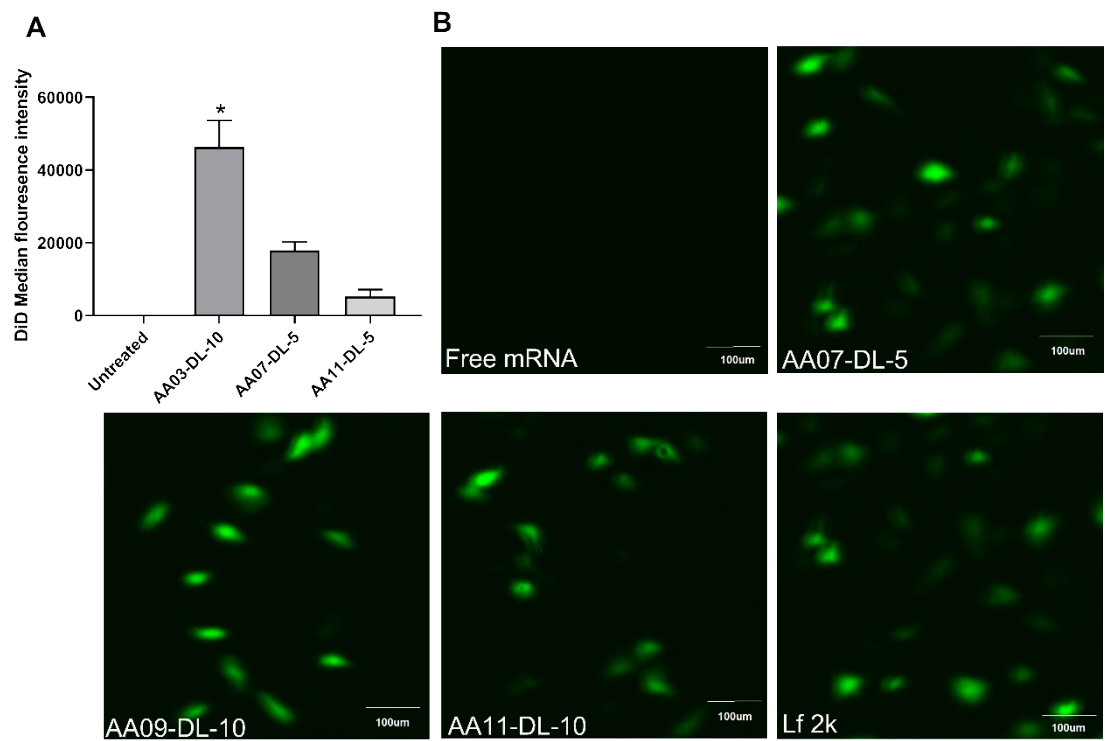


**Figure S29.** *In vitro* evaluation of  $\varepsilon$ -DL lipomers. (A) Flow cytometry analysis of cellular uptake of DiD labelled lipomers, 3 hours after incubation with HeLa cells. Data are presented as mean  $\pm$  SD; n = 3. (B) Representative images of EGFP expression in HeLa cells 8 hours after transfection with different lipomers. Scale bar represents 100  $\mu$ m. \*  $p < 0.001$ .

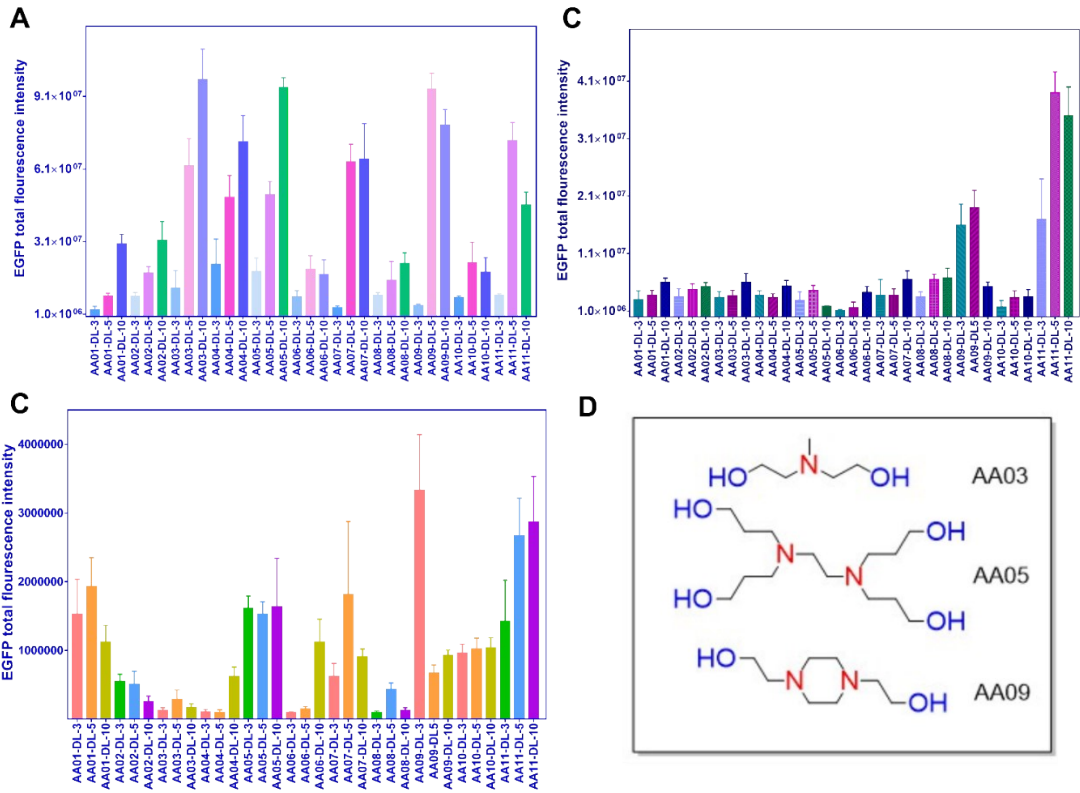


**Fig 30.** *In vivo* characterization of  $\varepsilon$ -DL combinatorial library. (A, B and C) EGFP expression efficiency in the main organs; lung, liver and spleen respectively, where ICR mice were injected at a dose of 0.25 mg/kg and organs were collected after 8 hrs, EGFP was quantified using flour vivo imaging system. (D) Chemical structures of the top performing initiators in vivo. Data presented as mean  $\pm$  SD; n = 3.

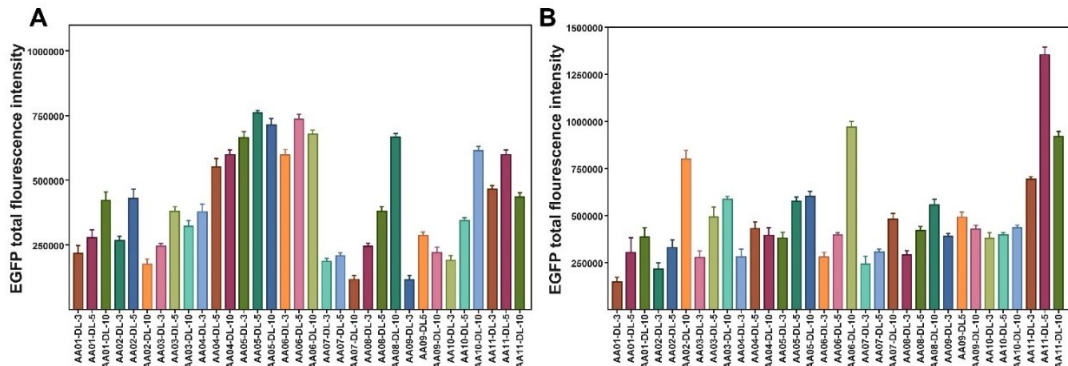


**Figure S31.** *In vivo* evaluation of  $\varepsilon$ -DL lipomers in heart (A) and kidneys (B). Mice were injected via tail vein with 0.25 mg/kg of  $\varepsilon$ -DL lipomers and EGFP fluorescence intensity was measured 8 hr after administration. Data presented as mean  $\pm$  SD; n = 3.

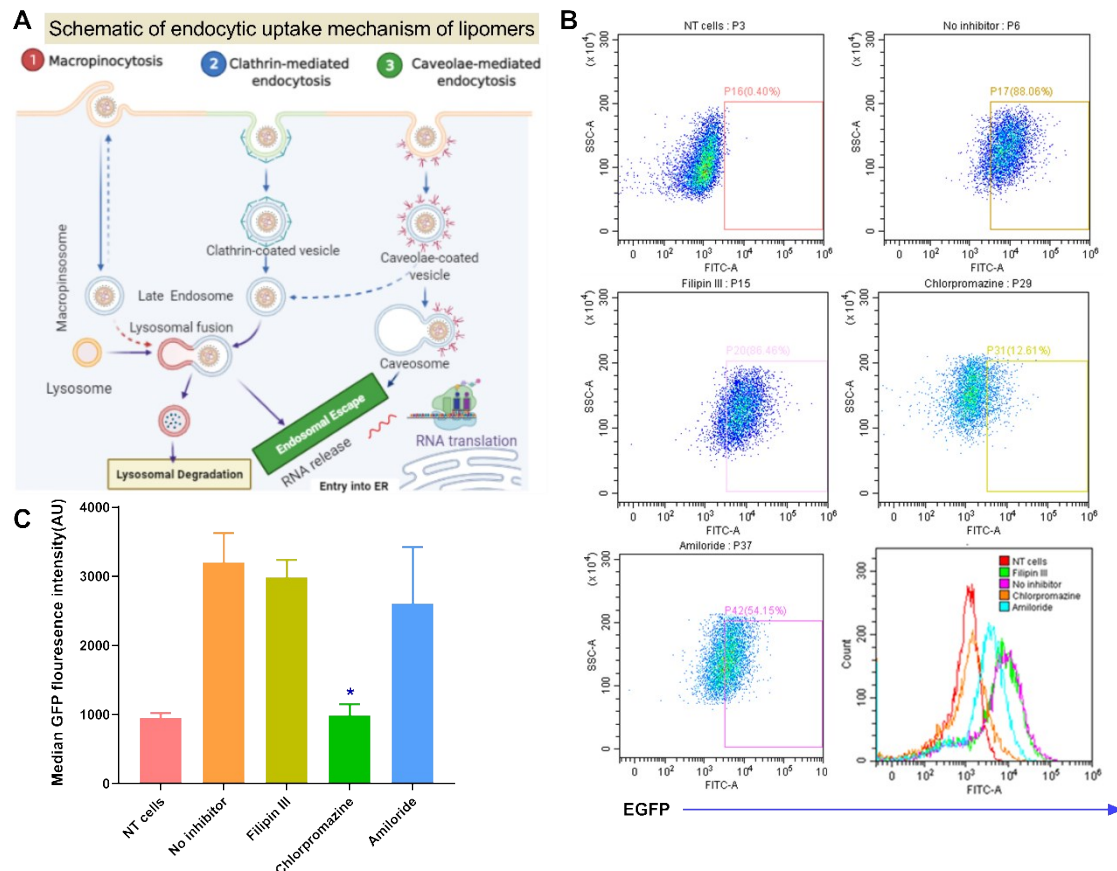


**Figure S32.** Uptake mechanism of the top performing lipomers at dose of 50 ng mRNA. (A) Schematic of the endocytic pathways for cellular uptake of lipomers (Adapted from Biorender.com). (B) EGFP transfection for different uptake inhibitors. (C) EGFP mean fluorescence intensity of different inhibitor treatments. Data presented as mean  $\pm$  SD; n = 3, \* p < 0.05.

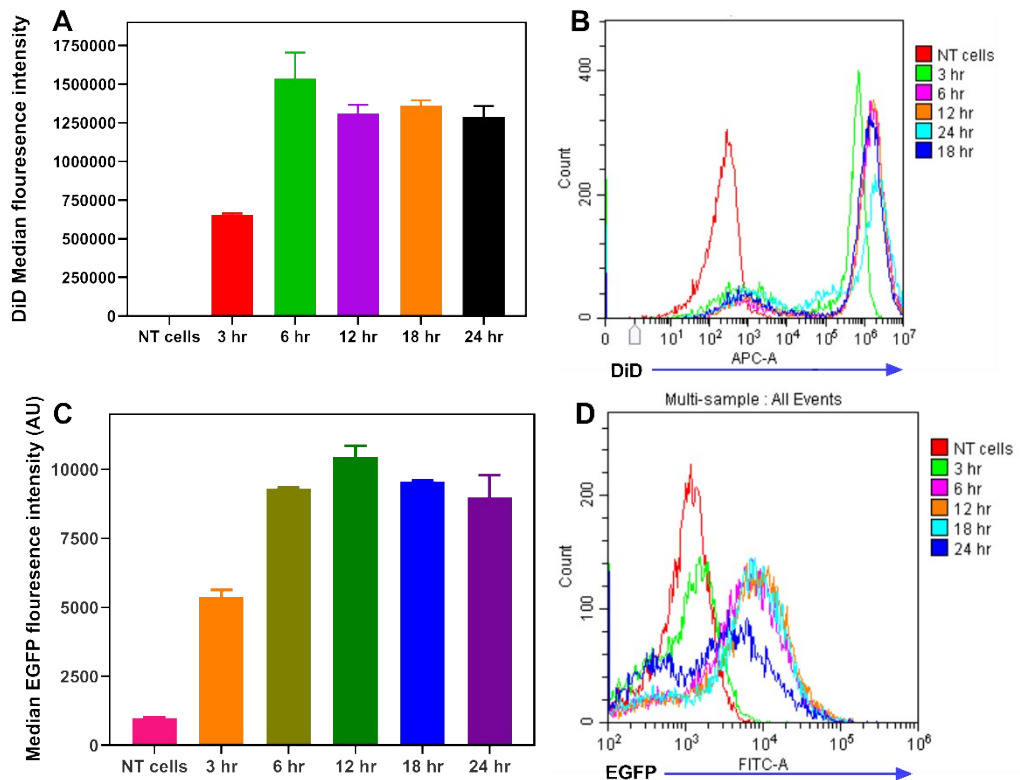


**Figure S33.** Dynamics of cellular uptake and mRNA expression of the top performing lipomers at dose of 100 ng mRNA per well. A) Cellular uptake of DiD labelled lipomers over 24 hr. B) flow cytometry histograms for the top performing lipomer over 24 hr. C) Dynamics of EGFP mRNA expression over 24 hr. D) Flow cytometry histogram of the top performing lipomer over 24 hr. Data presented as mean  $\pm$  SD; n = 3.

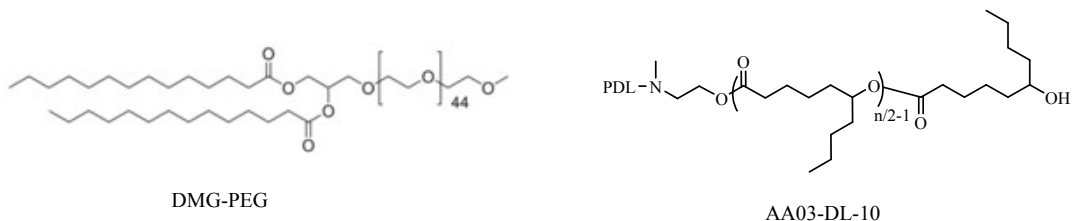


**Figure S34.** Schematic of the chemical structure of the two components of the top performing lipomer *in vivo*.

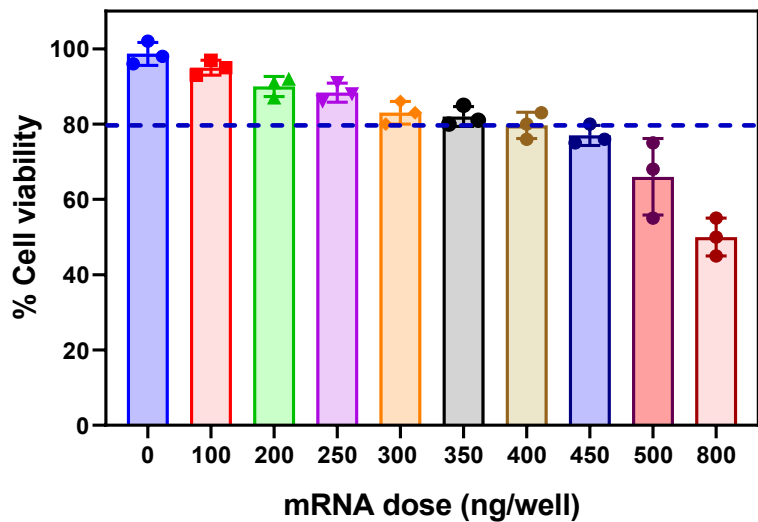


**Figure S35.** Relative viability of HeLa cells 24 hr after incubation with different doses AA03-DL-10 lipomers. Data presented as mean  $\pm$  SD; n = 3

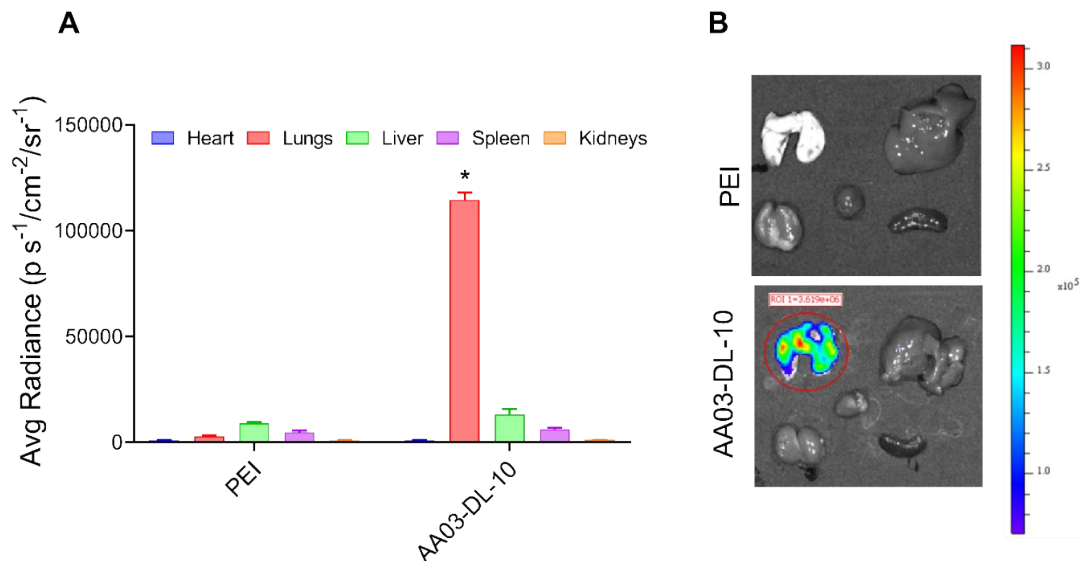


**Figure S36.** *In vivo* evaluation of the top performing lipomer (AA03-DL-10) compared to commercial PEI (A) and kidneys (B). Mice were injected via tail vein with 0.25 mg/kg of  $\epsilon$ -DL lipomers and EGFP fluorescence intensity was measured 8 hr after administration. Data presented as mean  $\pm$  SD; n = 3, \* p < 0.05.

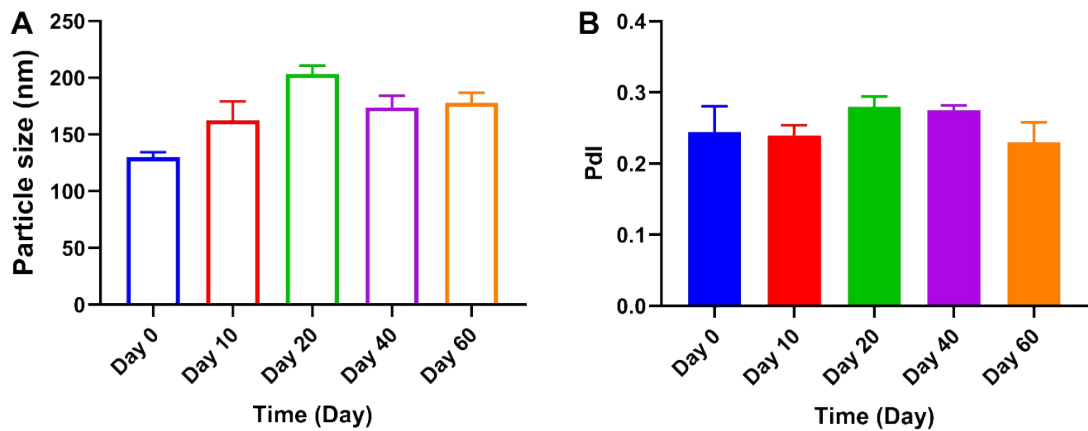


**Figure S37.** Long term stability of AA03-DL-10 lipomers. (A, B) Particle size and PDI were evaluated at Day 0, Day 10, Day 20, Day 40 and Day 60.

## References:

1. P. Hu, A. Greiner and S. Agarwal, *Journal of Polymer Science Part A: Polymer Chemistry*, 2019, **57**, 752-757.
2. S. Santiwarangkool, H. Akita, I. A. Khalil, M. M. Abd Elwakil, Y. Sato, K. Kusumoto and H. J. J. o. C. R. Harashima, 2019, **307**, 55-63.
3. M. A. Younis, I. A. Khalil, M. M. Abd Elwakil and H. Harashima, *Mol Pharm*, 2019, **16**, 4031-4044.